# Bioactive constituents of Verbena officinalis regulate killing efficiency of primary human natural killer cells by accelerating killing processes

**Rui Shao [1#], Xiangda Zhou [2#], Renping Zhao [2], Archana K. Yanamandra [2,3], Zhimei Xing [1], Xiangdong Dai [1], Han Zhang [1], Yi Wang [4], Yu Wang [1,5*], Bin Qu [2,3*]**

[1] State Key Laboratory of Component-based Chinese Medicine, Tianjin University of Traditional Chinese Medicine, Tianjin, China;

[2] Department of Biophysics, Center for Integrative Physiology and Molecular Medicine (CIPMM), School of Medicine, Saarland University, Homburg, Germany;

[3] Leibniz Institute for New Materials, Saarbrücken, Germany;

[4] Pharmaceutical Informatics Institute, College of Pharmaceutical Sciences, Zhejiang University, Hangzhou, China;

[5] School of Integrative Medicine, Tianjin University of Traditional Chinese Medicine, Tianjin, China.

[#] These authors contributed equally

*** Correspondence:**

**Bin Qu**
Department of Biophysics
Center for Integrative Physiology and Molecular Medicine (CIPMM)
School of Medicine, Saarland University
66421 Homburg, Germany.
Tel: +49 6841 16 16310, Fax: +49 6841 16 16302
Email: bin.qu@uks.eu

**Yu Wang**
School of Integrative Medicine
Tianjin University of Traditional Chinese Medicine
301617 Tianjin, China
Tel.: +86 22 59596171, Fax: +86 22 27493265
E-mail: wangyu@tjutcm.edu.cn

**Keywords:** NK cells, *Verbena officinalis* (*V. officinalis*), killing efficiency, innate immune system, Network pharmacological analysis.

**ABSTRACT**

*Background:* Natural killer (NK) cells play a key role in eliminating tumorigenic and pathogen-infected cells. *Verbena officinalis* (*V. officinalis*) has been used as a medical plant in traditional and modern medicine, exhibiting anti-tumor and anti-inflammation activity, but its role in NK cells remains unclear.

*Purpose:* The impact of bioactive constituents of *V. officinalis* on immune responses remains largely elusive. In this work we investigated the potential targets of *V. officinalis* and focused on killing efficiency and related functions of NK cells regulated by bioactive constituents of *V. officinalis*.

*Study design/methods:* We used primary human NK cells from peripheral blood mononuclear cells. Potential regulatory roles of selected compounds in NK killing function-related genes were first analyzed by network pharmacology approaches. Potential engagement between compounds and NK receptors was examined by molecular docking assay. Killing efficiency of NK cells was determined with real-time killing assay and live-cell imaging. Proliferation was examined by CFSE staining. Expression of cytotoxic proteins was analyzed using flow cytometry. Lytic granule release was quantified by CD107a degranulation assay. Contact time required for killing and determination of serial killers were analyzed using live cell imaging results.

*Results:* Results from network pharmacology approaches and molecular docking analyses predicted that the five bioactive compounds (acteoside, apigenin, kaempferol, verbenalin and hastatoside) from *V. officinalis* can regulated various key genes essential for NK effector functions and can bind to NK inhibitory receptors as well as activating receptors, indicating their potential role in regulating NK killing capacity. Analyses of NK killing efficiency revealed that out of these five compounds verbenalin exhibited an encouraging potency to enhance NK killing efficiency. Further investigation showed that verbenalin did not affect proliferation, expression of cytotoxic proteins, or lytic granule

degranulation, but rather reduced contact time required for killing, enhanced total killing events per NK cell, and elevated the fraction of killing competent NK cells.

*Conclusions:* In this work, we have identified verbenalin as the most potent bioactive constituent from *V. officinalis* to enhance NK cell killing efficiency via accelerating killing processes and converting non-killers to killing competent NK cells without affecting the lytic granule pathway.

## 1 Introduction

*Verbena officinalis* L. (*V. officinalis*), also known as common vervain, is a medicinal herb, widespread throughout the globe, mainly in the temperate climate zone (1). In China, *V. officinalis* is widely distributed in the southern part of the Yellow River and has been used as traditional Chinese medicine for the treatment of rheumatism, bronchitis, depression, insomnia, anxiety, liver and gallbladder diseases (1, 2). Recent reports suggest that *V. officinalis* has a number of scientifically proven activities, such as antioxidant, antibacterial, antifungal, anti-inflammatory, analgesic, anticonvulsant, anxiolytic, antidepressant, sedative, hypnotic, wound healing, gastro-protective, anti-cancer and insecticidal properties (1, 3-5). In addition to being used as an antimicrobial, secretolytic, expectorant and diuretic agent, *V. officinalis* is also widely used in food and cosmetics, especially due to its antioxidant, antibacterial, and anti-inflammatory properties (1).

*V. officinalis*, blooming overground parts of the plant, contains flavonoids, terpenoids, phenolic acids, phenylpropanoids and iridoids (1, 2, 6, 7). Verbenalin and hastatoside, belonging to iridoids, are characteristic constituents of *V. officinalis*, and they exhibit various biological activities including sleep-promoting, antioxidant, and hepatoprotective activity (6). Moreover, the relative content of Verbenalin and hastatoside are higher compared to that of other characteristic iridoids in *V. officinalis*, serving as promising target constituents for quality control of *V. officinalis*. Kaempferol and apigenin represent the most encountered aglycone flavonoids isolated from *V. officinalis* Kaempferol has been

shown to be cardioprotective, neuroprotective, anti-inflammatory, anti-diabetic, anti-oxidant, anti-microbial, and have anticancer activities (8). Acteoside, belonging to phenylpropanoid glycosides, is water-soluble and exhibits a wide range of biological activities, such as anti-tumor, anti-microbial, anti-inflammatory, anti-thrombotic and wound healing properties (9). The regulatory role of *V. officinalis* on functions of immune cells is not well understood. Recently, it is reported that the extracts from *V. officinalis* do not exhibit significant effect on macrophages and neutrophils (10). In this work, we were mainly focused on natural killer (NK) cells.

NK cells are specialized immune killer cells belonging to innate immune system, which play a key role in eliminating transformed and pathogen-infected cells (11). Activation of NK cell killing function is regulated by an integrated output of intracellular signals triggered by activating and inhibitory surface receptors. Major activating receptors in humans are natural cytotoxicity receptors (e.g. NKp46, NKp44 and NKp30) and a C-type lectin-like receptor NKG2D (12). NK activating receptors recognize stress-induced ligands or the molecules induced upon transformation or viral infection (13, 14). Inhibitory receptors engage with major histocompatibility complex (MHC) Class I molecules, which are expressed on all healthy cells to distinguish non-self or aberrant cells (15). NKG2A form heterodimers with CD94 (16), serving as one of the most prominent inhibitory receptors in NK cells (17). A few killer cell immunoglobulin-like receptors (KIRs) also conduct inhibitory function in NK cells (18).

To successfully execute their killing function, NK cells need to infiltrate into tissues to search for their target cells. Once the target cells are identified, a tight junction termed the immunological synapse (IS) will be formed between the NK cell and the target cells (19). Consequently, cytotoxic protein-containing lytic granules (LGs) in NK cells are enriched and released into the cleft at the IS (20). Cytotoxic proteins in LGs are mainly the pore-forming protein perforin and the serine proteases granzymes. In LGs, activity of perforin is inhibited mainly by the acidic pH (21). Upon release, perforin

oligomerizes and forms transient pores on the plasma membrane of target cells to facilitate entry of granzymes into target cells or induce direct lysis of target cells (21). Granzymes mainly function via cleavage of caspases to trigger downstream cascades resulting in apoptosis of target cells (22).

In this work, we aimed to investigate regulation of NK killing efficiency by active constituents of *V. officinalis* and the underlying mechanisms. We were focused on five compounds (acteoside, apigenin, kaempferol, verbenalin and hastatoside) from *V. officinalis.* Using network pharmacology approaches, we identified several genes essential for NK functions that could be regulated by these compounds. Results from molecular docking assay predicted that these constituents could bind to NK inhibitory and activating receptors. Using real-time killing assay, we found that NK killing efficiency was decreased after treatment with acteoside, apigenin, or kaempferol, and enhanced substantially by verbenalin and to a lesser extent by hastatoside. Verbenalin-enhanced NK killing efficiency was also confirmed in 3D collagen. We revealed that treatment with verbenalin shortened the duration required for NK-induced target death and increased the fraction of killing competent NK cells, especially serial killers, without affecting the lytic granule pathway.

## 2 Article types

Original Research.

## 3 Manuscript Formatting

### 3.1 Materials and Methods

***Reagents and antibodies***

The following reagents were used: acteoside, apigenin, kaempferol, verbenalin and hastatoside were purchased from Shanghai Winherb Medical Technology Co., Ltd with a purity greater than 98%, carboxyfluorescein succinimidyl ester (CFSE, Thermo Fisher Scientific), calcein-AM (Thermo Fisher Scientific), protein transport inhibitor GolgiStop (BD Biosciences), bovine collagen type I solution (Advanced Biomatrix), and recombinant human IL-2 (Miltenyi Biotec). The antibodies were purchased

from Biolegend: Alexa 488 anti-human CD3 antibody, APC anti-human CD56 antibody, PerCP anti-human CD16 antibody, PerCP/Cyanine5.5 anti-human Granzyme B antibody, and Brilliant Violet 510 anti-human perforin antibody, and Brilliant Violet 421 anti-human CD107a antibody.

***Network pharmacological analysis***

Prediction of targets of five representative components of *V. officinalis* was performed by TCMSP, TCM-MESH, Symmap, and TCMID database. We constructed a PPI (protein–protein interaction) network to elucidate the molecular mechanisms of effects of *V. officinalis* by using the Cytoscape software (version 3.7.2; http://www.cytoscape.org) and the STRING database (version 11.0, http://www.string-db.org/) with a required confidence >0.4. Next, the degree of connectivity in the PPI network was analyzed by Cytoscape software (version 3.7.2) and the top 20 hub genes were obtained. We used online tools such as GeneCards (http://www.genecards.org/) to find potential targets for NK cell-mediated cytotoxicity. Venn Diagram (http://bioinformatics.psb.ugent.be/webtools/Venn/) was used to find overlapping genes between potential targets of *V. officinalis* and NK cell-mediated cytotoxicity related targets.

***Molecular Docking***

To investigate the interactions between small molecules and receptor proteins, the CDOCKER module in Discovery Studio software was used for molecular docking. The three-dimensional structures of five small molecules were download from TCMSP （https://tcmsp-e.com/ ）, and then perform hydrogenation through the Prepare Ligand module, optimize the energy with CHARMM force field. The three-dimensional structure of target protein was downloaded from the PDB database (https://www.rcsb.org/). Then run the Prepare Protein module to optimize the protein structure: delete redundant protein conformations, delete water molecules, complete incomplete residues, hydrogenation and distribution of related charges. The prepared target proteins and small molecules

were introduced into Discovery Studio and docked using CDOCKER module. The semi flexible docking method and simulated annealing algorithm are used to find the optimal conformation of ligand and receptor. And according to the level of CDOCKER Interaction Energy to evaluate the degree of docking, the lower the scoring function value, the stronger the affinity of the small molecule with the receptor.

***NK Cell preparation and cell culture***

Human primary NK cells were isolated from peripheral blood mononuclear cells (PBMCs) of healthy donors using Human NK Cell Isolation Kit (Miltenyi Biotec). The isolated NK cells were cultured in AIM V medium (Thermo Fischer Scientific) with 10% FCS and 100 U/ml of recombinant human IL-2 for three days prior to the experiments. For the conditions with compound treatment 10 μM and 30 μM of each compound was added into the medium along with IL-2 for three days. K562 and K562-pCasper cells were cultured in RPMI-1640 medium (Thermo Fischer Scientific) with 10% FCS. For K562-pCasper cells, 1.25mg/ml G418 was added. All cells were kept at 37 °C with 5% $CO_2$.

***Real-time killing assay***

Real-time killing assay was conducted as reported previously (23). Briefly, target cells (K562 cells) were loaded with Calcein-AM (500 nM) and settled into a 96-well plate ($2.5\times10^4$ target cells per well). NK cells were subsequently added with an effector to target (E:T) ratio of 2.5:1. Fluorescence intensity was determined by GENios Pro micro-plate reader (TECAN) using the bottom-reading mode at 37°C every 10 min for 4 hours. Target lysis (t) % = $100 \times (F_{live}(t)-F_{exp}(t))/(F_{live}(t)-F_{lysed}(t))$. (F: fluorescence intensity)

***3D live cell imaging***

As described previously (24), K562-pCasper target cells were resuspended in 2 mg/ml of pre-chilled neutralized Bovine type I collagen solution in a half-area well flat clear bottom black 96 well plate (Corning) ($1.25\times10^4$ cells in 20 µl per well). The collagen was solidified at 37°C with 5% $CO_2$ for 40 min. NK cells were subsequently put on top of collagen as effector cells with an E:T ratio of 2.5:1. The killing events were visualized using ImageXpress Micro XLS Widefield High-Content Analysis System (Molecular Devices) at 37°C with 5% $CO_2$. Images of FRET signal, GFP signal and brightfield were obtained. For 3D killing assay, the killing events were visualized every 20 minutes for 36 hours, and numbers of live target cells were normalized to hour 0 based on the area detected in FRET channel. To determine time required for killing and the average kills per NK cell, images were acquired every 70 seconds for 14 hours. The NK cells that killed at least one target were selected for further analysis. NK cells were tracked manually to identify the time point of establishing contact and apoptosis, which is used to determine Contact-Apoptosis Time. Induction of target apoptosis (loss of FRET signal) or direct lysis (simultaneous loss of FRET and GFP signal) was defined as kills. To determine fractions of serial- (kills per NK > 1), single- (kills per NK = 1), and non-killer (kills per NK = 0), NK cells were randomly selected and tracked. Image J software (https://imagej.nih.gov/ij/) was used to process and analyze the images.

***Proliferation assay***

Freshly isolated primary human NK cells were labelled with CFSE (5 µM) in PBS with 5% FCS at a density of $1\times10^6$/ml at room temperature for 15 minutes followed by one wash with AIMV medium. CFSE-loaded NK cells were stimulated with recombinant human IL-2 (100 U/ml) in presence of verbenalin or DMSO in AIMV (10% FCS) at 37ºC with 5% $CO_2$ for 3 days. Primary human NK cells without CFSE staining were used as negative control to gate CFSE positive cells. Fluorescence of CFSE was determined with a FACSVerse™ flow cytometer (BD Biosciences) and analyzed with FlowJo v10 (FLOWJO, LLC).*4.7.*

### *Determination of cytotoxic protein expression*

To test perforin and granzyme B expression, negatively isolated primary human NK cells were cultured in presence of IL-2 (100 U/ml) and the corresponding compound at the desired concentration indicated in the figures. NK cells were fixed on day 3 in pre-chilled 4% paraformaldehyde. Permeabilization was carried out using 0.1% saponin in PBS containing 0.5% BSA and 5% FCS, followed by staining with Alexa 488 anti-human CD3 antibody, APC anti-human CD56 antibody, PerCP/Cyanine5.5 anti-human Granzyme B antibody, and Brilliant Violet 510 anti-human perforin antibody in PBS (containing 0.1% saponin, 0.5% BSA and 5% FCS) at room temperature for 30 minutes. NK cells were then washed twice and resuspended in PBS containing 0.5% BSA prior to flow cytometry analysis with FACSVerse™ flow cytometer (BD Biosciences). $CD3^{-}CD56^{+}$ cells were gated as NK cells. FlowJo v10 (FLOWJO, LLC) was used for analysis.

### *CD107a degranulation assay*

For degranulation assay, NK cells were settled with K562 cells at a ratio of 2.5:1 in presence of Brilliant Violet 421 anti-human CD107a (LAMP1) antibody and GolgiStop™ in a flat bottom 96-well plate (Corning, 50 µl/well) for 4 hours at 37°C with 5% $CO_2$. The supernatant was removed, and the cell mix was stained with PerCP anti-human CD16 antibody and APC mouse anti-human CD56 antibody at room temperature for 30 minutes. The cell mix was washed twice and resuspended in PBS containing 0.5% BSA prior to flow cytometry analysis with a FACSVerse™ flow cytometer (BD Biosciences). $CD56^{+}CD16^{+}$cells were gated as NK cells. Results were analyzed with FlowJo v10 (FLOWJO, LLC).

### *Statistical analysis*

GraphPad Prism 6 Software (San Diego, CA, USA) was used for statistical analysis. If the number of data points is smaller than 8, the differences between two columns were analyzed by the Student's t-

test (paired or unpaired as indicated in the figure legends). If the number of data points is greater than 8, for normally distributed datasets, unpaired Student's t-test was conducted; for the datasets that did not pass normality test, Mann-Whitney test was applied.

## Results

### *Assessment of possible regulatory roles of V. officinalis bioactive ingredients in NK functions*

To explore the pharmacological mechanism of *V. officinalis* on NK killing-related processes, five compounds (acteoside, apigenin, kaempferol, verbenalin and hastatoside) were selected as bioactive ingredients based on the TCMSP, TCM-MESH, Symmap, and TCMID database analyses (Figure 1A). Then, potential targets of these five ingredients were predicted via the SwissTargetPrediction database based on their structure, and a total of 117 targets were obtained (Supplementary Figure 1). Concerning possible molecules and pathways NK killing-related processes, we retrieved a total of 2489 genes from the GeneCards databases in this aspect. A total of 71 potential targets of *V. officinalis* on NK mediated cytotoxicity were obtained as shown in the Venn diagram (Figure 1B). The corresponding PPI network of *V. officinalis* ingredient–NK target is shown in Figure 1C, where the size of the nodes positively correlates with their degree. We noticed that the largest nodes such as AKT1, TP53, JUN, and TNF play essential roles in NK effector functions.

In addition, we analyzed whether active compounds of *V. officinalis* could bind to NK inhibitory or activating surface receptors. To this end, we selected several major players including four activating receptors (NKG2D, NKp30, NK44, and NKp46) and two inhibitory receptors (NKG2A and KIR2DL1). Results from molecular docking analysis predict that among activating receptors, NKp46 could not interact with any of the five continents, NKp30 could engage with all five, NKp44 with four but acteoside, NKG2D with apigenin and kaempferol (Figure 2A, supplementary Table 1). In comparison, among inhibitory receptors, NKG2A could engage with three bioactive compounds

(apigenin, kaempferol, and verbenalin), and KIR2DL1 can interact with all five (Figure 2B, Supplementary Table 2). These data indicate that *V. officinalis* bioactive constituents could be involved in regulating NK functions, especially the killing-relevant processes.

***Impact of bioactive components of V. officinalis on NK killing efficiency***

To verify the impact of bioactive constituents of *V. officinalis* on NK killing efficiency, we cultured primary human NK cells with the corresponding compound at two concentrations (10 µM and 30 µM) for three days in presence of IL-2. We used K562 cells, a chronic myeloid leukemia cell line, as target cells. K562 cells were loaded with fluorescent dye calcein-AM and loss of fluorescence due to NK killing was determined using a microplate-reader at 37ºC every 10 minutes for 4 hours (23). We found that NK killing efficiency was slightly reduced by acteoside, apigenin, and kaempferol, but enhanced by verbenalin and hastatoside (Figure 3A). Verbenalin exhibited the highest potency for elevation of NK killing efficiency (Figure 3A). We further verified the impact of verbenalin on NK killing efficiency in 3D for longer term up to 36 hours. To visualize killing events, K562 cells expressing FRET-based apoptosis reporter pCasper (K562-pCasper) were used. GFP-RFP FRET pair is linked by a caspase recognition site (DEVD). Living K562-pCasper target cells exhibit orange/yellow color originated from the red FRET signal and the green GFP signal; when K562-pCasper undergo apoptosis, the DEVD linker is cleaved by activated caspases, resulting in loss of FRET signal, thus apoptotic K562-pCasper cells would turn green (25). For long term 3D killing assay, K562-pCasper target cells were embedded in 3D collagen matrix and NK cells were added from the top. With live-cell imaging for 36 hours we observed that NK cells treated with verbenalin of 10 µM or 30 µM initiated killing much earlier than the control NK cells (Figure 3B), and verbenalin-treated NK cells exhibited significantly faster killing kinetics compared to their counterparts treated with vehicle (Figure 3C). Noticeably, numbers of target cells were slightly enhanced within the first 12 hours likely due to cell

proliferation. Taken together, we conclude that among the bioactive constituents of *V. officinalis*, Verbenalin substantially increase NK killing efficiency under a physiologically relevant 3D condition.

***Verbenalin accelerates NK killing processes and enhanced the fraction of killing competent NK cells***

Next, we sought for the underlying mechanisms of increase in NK killing efficiency by verbenalin. First, we examined proliferation using CFSE-loaded NK cells. On day 3 after IL-2 stimulation, no difference was detected between verbenalin-treated and DMSO-treated NK cells (Figure 4A). Since lytic granule pathway is essential for NK killing capability, we next analyzed expression of cytotoxic proteins (perforin and granzyme B). Flow cytometry analyses show no alteration in protein levels of perforin or granzyme B by verbenalin treatment (Figures 4B, C). As lytic granule release is a key step for NK cells to execute their killing function, we analyzed degranulation using CD107a, also known as lysosomal-associated membrane protein 1, which is integrated into the plasma membrane of NK cells after lytic granule release. NK cells were co-incubated with K562 cells for four hours to trigger degranulation and fluorescently labeled CD107a antibody was present in the media along with GolgiStop to inhibit internalization of CD107a. We found that the fraction of $CD107a^{+}$ NK cells was similar for verbenalin-treated NK cells compared to control NK cells (Figure 4D). These results indicate that canonical lytic granule pathway in NK cells is not affected by verbenalin.

We next analyzed three parameters related to killing efficiency including the duration required for death induction, average kills per NK cell, and fraction of killing competent NK cells. Killing events were visualized with high-content imaging setup every 70 sec for 12 hours (Figure 5A, Movie 1). We observed that NK cells induced both target cell apoptosis as indicated by sudden loss of FRET signal with remaining GFP signal (Figure 7A, Movie 1, Target #1 in Ctrl and Target #2/#3 in verbenalin) and direct lysis as indicated by simultaneous loss of FRET and GFP signal (Figure 5A, Target #1 in verbenalin). Both cases were considered as target cell death. We then analyzed the durations between

contact formation and induction of target cell death. We found that this duration was reduced in verbenalin-treated NK cells in relative to their vehicle-treated counterparts for donor 1; donor 2 showed the same tendency but the difference was not statistically significant (Figure 5B). Concomitantly, on average, the numbers of target cells killed per NK cell was almost doubled for Verbenalin-treated NK cells relative to their counterparts for donor 1 and to a lesser extent for donor 2 (Figure 5C). We These data indicate that treatment with verbenalin can accelerate killing processes of NK cells and result in more killing events mediated by NK cells.

We noticed that NK cells fell into three categories: serial killers that could kill more than one target cell (Figure 5A, Movie 1, NK in the verbenalin panel), single killer that could only kill one target cells (Figure 5A, Movie 1, NK in the Ctrl panel), and non-killers that did not kill any target cell. We analyzed the fractions of these three categories and found that treatment with verbenalin substantially reduced the portion of non-killers and concomitantly enhanced the fraction of serial killers (Figure 5D). This result suggests that less killing competent NK cells are transformed to more killing competent NK cells after treatment with verbenalin.

## Discussion

In our work, we assessed possible impact of bioactive constituents of *V. officinalis* on NK cell functions using network pharmacology approaches and molecular docking. The results predicted that *V. officinalis* constituents (acteoside, apigenin, kaempferol, verbenalin and hastatoside) could regulate an array of genes essential for NK effector function (e.g. Akt1, NFκB, JUN, TNF, IFNγ, and IL-2) and could bind to NK surface receptors. Further functional assays show that among the five *V. officinalis* constituents, only verbenalin significantly elevated NK killing efficiency. Nevertheless, proliferation of NK cells was not affected by verbenalin. Expression of cytotoxic proteins (perforin and granzyme B) and degranulation of lytic granules stayed unaltered by verbenalin treatment. Unexpectedly, we

found that verbenalin accelerated NK killing processes, elevated average kills per NK. More interestingly, verbenalin reduced the fraction of non-killers and elevated the fraction of serial killers.

The duration required for NK cells to complete killing is decided by at least five steps: recognition of target cells, establishment of the contact, re-orientation of killing machinery, lytic granule release, death induction in target cells. Target recognition is dependent on an integrated outcome of activation of activating receptors and weakened signal from inhibitory receptors. Establishing the contact requires engagement of adhesion molecules, predominantly between lymphocyte function-associated antigen 1 (LFA-1) on NK cells and intercellular adhesion molecule 1 (ICAM-1) on target cells. Upon contact formation, the microtubule-organizing center (MTOC) is re-oriented towards the IS and lytic granules are transported along microtubules towards the IS (19). Subsequently, lytic granules are docked on and fused with the plasma membrane, which is highly dependent on SNARE proteins and calcium influx (20). In some cases, perforin-formed pores on target cell plasma membrane are sufficient to lyse target cells, but more often, target cell destruction is mediated by granzyme-induced apoptosis (25). We do not have direct evidence for which steps are accelerated by verbenalin. Nevertheless, our results from network pharmacology analysis and molecular docking could provide a few hints. Bioactive component of *V. officinalis* is predicted to regulate CD40LG (CD40 ligand) and CD40 signaling is reported to be involved in activation of LFA-1 in NK cells (26), which is essential for NK activation (27). Of note, adhesion molecules ICAM-1 and VCAM-1 are among the top hits from network pharmacology analysis, which could also eventually affect establishment of contact. Potential engagement between verbenalin and activating receptors NKp30 and NKp44 as well as inhibitory receptors NKG2A and KIR2DL1 are predicted by molecular docking analysis. K562 cells are MHC-I molecule-deficient, therefore signaling cascades downstream of inhibitory receptors should not be elicited. The activating receptors could be therefore possible candidates for verbenalin to shorten the step of target recognition. Furthermore, it is reported that CD40 ligand-expressing NK cells can induce

destruction of $CD40^+$ target cells via CD40 ligand/CD40 interaction (28) and K562 cells express considerably amount of surface CD40 (29). CD40 ligand could serve as another possible target for verbenalin to accelerate killing. As in verbenalin-treated NK cells no alteration in lytic granule pathway was identified, any impact of verbenalin on the steps of re-orientation of killing machinery, lytic granule release, and death induction in target cells to shorten the duration required for killing seems to be unlikely.

How many target cells one NK cell can kill is dependent on three major factors: how fast the NK cell can find its targets, how much time it spends on the targets, and the availability of lytic granules. As K562 cell line does not express FAS (CD95) (30), Fas/FasL pathway cannot play any role in verbenalin-enhanced NK killing efficiency. Efficiently locating target cells relies on proper motility and optimal searching strategies. NK cell motility is highly dependent on rearrangement of cytoskeleton and activity of cytoskeleton related kinases (31). Top hits from our network pharmacology analysis do not include any cytoskeleton or related genes and we did not observe changes in NK cell migration. Concerning the duration NK cells spend on the target cells, we observed that some verbenalin-treated NK cells detached target cells even before the apoptosis was initiated (Figure 5A, target #2/#3 in the verbenalin panel), whereas control NK cells detached their targets normally a few minutes after initiation of apoptosis (Figure 3A, target #1 in the Ctrl panel). Considering that the duration between establishing contact and target cell death for NK cells was reduced by verbenalin treatment, the duration for NK cells being conjugated with target cells should be corresponding reduced in verbenalin-treated NK cells. Numbers of target cells one NK can kill should be positively correlated to the numbers of lytic granules, at least to certain extent. Since the cytotoxic protein expression and lytic granule release are not affected by verbenalin, possibilities for verbenalin to alter numbers of lytic granules in NK cells are low but cannot be excluded.

In this work, we found that treatment with verbenalin considerably reduced the percentage of non-killer NK cells, indicating that a fraction of non-killers is converted to killing competent NK cells by verbenalin. Why some NK cells behave as non-killers? At least two possibilities: expression levels of cytotoxic proteins are too low and/or surface checkpoint molecules hinder killing. Concerning cytotoxic protein levels, no difference was identified between verbenalin-treated and control NK cells after three days of IL-2 stimulation. We hypothesize that cytotoxic proteins could be newly synthesized upon conjugating with the target cells. This hypothesis is supported by a previous work showing that in cytotoxic T lymphocytes (CTLs), 5 minutes after IS formation, new lytic granules can be produced at a rate of 1 granule per minute as predicted by experimental data-based compartment models (32). Network pharmacology analysis in this work predicts the transcription factor NFκB as a top hit. NFκB plays a major role in regulating expression of perforin and granzyme B (33, 34). Concerning checkpoint molecules, it is reported that after encountering K562 cells, primary human NK cells significantly up-regulated PD-L1 expression at mRNA and protein levels (35). The transcription factor c-Jun is essential for PD-L1 expression (36). As one top hits from network pharmacology analysis, c-Jun could be another target molecule for verbenalin to convert non-killer NK cells to a killing competent status. Future efforts are required to identify the corresponding underlying molecular mechanism.

*V. officinalis* has a long tradition being used as a medical herb throughout the world, e.g. in Europe, Asia, American and Australia (1, 37). Anti-tumor activity of *V. officinalis* has been reported (38). Recently, a newly developed formula XuanFeiBaiDu composed of thirteen medical herbs including *V. officinalis* has shown encouraging clinical outcome treating COVID-19 patients (39), and a potent effect on dampening macrophage-mediated inflammatory responses (10). In this work, we have established a direct link between verbenalin, a bioactive constituent of *V. officinalis*, and killing efficiency of NK cells, adding to our understanding of the regulatory effect of *V. officinalis* on the killing effectiveness of primary human natural killer cells.

## 3.2 Figure legends

**Figure 1. Target genes of *V. officinalis* and NK and their network.** (A) The five bioactive ingredients from *V. officinalis*. (B) Venn diagram of overlapping genes between *V. officinalis* regulated and NK function related genes. A total of 2489 targets were retrieved from the GeneCards database. Venn diagram analysis (http://bioinformatics.psb.ugent.be/webtools/Venn/) was conducted. (C) Top hub genes in NK cells regulated by the five bioactive ingredients from *V. officinalis*. PPI network was analyzed using Cytoscape software and the STRING database with a required confidence >0.4. The degree of connectivity in the PPI network was analyzed by Cytoscape software to obtain the top 20 hub genes.

**Figure 2. Molecular docking between *V. officinalis* bioactive constituents and NK surface receptors.** The 3D structures of the constituents and target receptors were download from TCMSP and PDB database, respectively. Following activating receptors (NKp46/1P6F, NKp30/3NOI, NKp44/1HKF, and NKG2D/1fMPU) and inhibitory receptors (NKG1A/3BDW and KIR2DL1/1IM9) were analyzed. The structures were optimized as described in the Methods. The CDOCKER module in Discovery Studio software was used for the analysis. The semi flexible docking method and simulated annealing algorithm are used to find the optimal conformation of ligand and receptor. Negative interaction energies indicate possible engagement. Schematic 3D represented the molecular docking model and active sites of the corresponding constituents with activating receptors and inhibitory receptors are shown in **A** and **B**, respectively.

**Figure 3. Bioactive constituents of *V. officinalis* differentially regulate NK killing efficiency.** Negatively isolated primary human NK cells were stimulated with IL-2 in presence with the corresponding compound for three days prior to experiments. DMSO was used as control (Ctrl). (A) Kinetics of NK killing affected by *V. officinalis* bioactive constituents. K562 cells were used as target cells with an effector to target (E:T) ratio of 2.5:1. K562 cells were loaded with calcein-AM. Target

cell fluorescence were determined with a microplate reader using the bottom-reading mode at 37ºC every 10 minutes for 4 hours. Results are from four donors. One representative donor is shown for each compound. Aceoside, apigenin and kaempferol were examined in parallel and shared the same DMSO control. (B, C) Verbenalin enhances NK killing efficiency in 3D. K562-pCasper cells were embedded in bovine type I collagen (2 mg/ml). NK cells were added from top with an E:T ratio of 2.5:1. Live cell imaging was acquired with a high content imaging system ImageXpress at 37ºC with 5% $CO_2$ every 20 minutes for 36 hours. Selected time points are shown in **B** and the quantification of live target cells is shown in **C**. One representative donor out of four is shown.

**Figure 4. Proliferation and lytic granule pathway of NK cells are not affected by verbenalin.** Primary human NK cells were stimulated with IL-2 in presence of verbenalin at the with indicated concentrations for 3 days prior to experiments. (A) Proliferation of NK cells. NK cells were stained with CFSE directly after isolation. Fluorescence was analyzed with flow cytometry on day 3. One representative donor out of four is shown. (B, C) Expression of cytotoxic proteins. On day 3, NK cells were fixed, permeabilized and stained with Alexa 488 anti-human CD3 antibody, APC anti-human CD56 antibody, PerCP/Cyanine5.5 anti-human Granzyme B antibody, and Brilliant Violet 510 anti-human perforin antibody. $CD3^{-}CD56^{+}$ cells were gated as NK cells. Expression of perforin (**B**) and granzyme B (**C**) was determined by flow cytometry. MFI: mean fluorescence intensity. Results are from four donors. (D) Release of lytic granules is not affected by verbenalin. CD107a degranulation assay was used to determine lytic granule release. NK cells and K562 cells were co-incubated in a flat bottom 96-well plate at an E:T ratio of 2.5:1 at 37ºC with 5% $CO_2$ for 4 hours in presence with Brilliant Violet 421 anti-human CD107a (LAMP1) antibody and GolgiStop. Results are from four donors. ns: not significant ($p > 0.5$). Paired Student's t-test was used for statistical analysis.

**Figure 5. Verbenalin shortens the time required for killing and elevates the fraction of killing competent NK cells.** Primary human NK cells were stimulated with IL-2 in presence of verbenalin at

30 μM for 3 days prior to experiments. DMSO was used as the vehicle control. K562-pCaspar target cells were embedded in collagen (2 mg/ml) and NK cells were added from top. Killing events were visualized at 37°C every 70 seconds for 14 hours. (**A**) Time lapse of 3D killing. One representative NK cell from each condition is shown. NK cells (red) were not fluorescently labeled. NK-conjugated target cells are sequentially numbered. Time stamp is shown as HH:MM:SS. Scale bars are 20 μm. (**B**) Verbenalin shortens the duration required for killing. The time required from NK cell touching the target till target lysis was quantified. Only NK cells that successfully killed at least one target cell were included. (**C, D**) Verbenalin potentiates NK killing possibility. NK cells were randomly chosen and manually tracked. Number of target cells killed per NK cell is shown in **C**. Fractions of serial killer (kills > 1), single killer (kills = 1) and non-killer (kills = 0) are shown in **D**. Results are from two donors. 21 NK cells were randomly chosen from each condition in **C** and **D**. Mann-Whitney test was used for statistical analysis.

## 4 Conflict of Interest

The authors declare that the research was conducted in the absence of any commercial or financial relationships that could be construed as a potential conflict of interest.

## 5 Ethics statement

Research carried out for this study with healthy donor material (leukocyte reduction system chambers from human blood donors) is authorized by Ethik-Kommission bei der Ärztekammer des Saarlandes (Identification Nr. 84/15, Prof. Dr. Rettig-Stürmer; Amendment approved on 23.03.2021, Prof. Markus Hoth).

## 6 Author Contributions

YW and BQ generated ideas and designed experiments. XZ performed most experiments. RZ and AY performed experiments for Figs. 4B, C. RS conducted the network pharmacology analysis. ZX

conducted the molecular docking verification. RS, YW and BQ wrote the manuscript. All authors contributed to the article and approved the submitted version.

## 7 Funding

This project was funded by National Key R&D Program of China (No. 2021YFE0200300 to Y.W., and No. 2020YFA0708004 to H.Z.), by Tianjin University of Traditional Chinese Medicine (No.YJSKC-20211015),by the Deutsche Forschungsgemeinschaft (SFB 1027 A2 to B.Q., Forschungsgroßgeräte (GZ: INST 256/423-1 FUGG for the flow cytometer, and GZ: INST 256/429-1 FUGB for ImageXpress), and by the Leibniz-Gemeinschaft (INM Fellow to B.Q.).

## 8 Acknowledgments

We thank the Institute for Clinical Hemostaseology and Transfusion Medicine for providing donor blood; Carmen Hässig, Cora Hoxha, and Gertrud Schäfer for excellent technical help, Markus Hoth and Eva C. Schwarz for K562-pCasper cells and inspiring discussion.

## 9 References

1. Kubica P, Szopa A, Dominiak J, Luczkiewicz M, Ekiert H: Verbena officinalis (Common Vervain) - A Review on the Investigations of This Medicinally Important Plant Species. *Planta Med* (2020), 86**:**1241-1257. doi: 10.1055/a-1232-5758.
2. Khan AW, Khan AU, Ahmed T: Anticonvulsant, Anxiolytic, and Sedative Activities of Verbena officinalis. *Front Pharmacol* (2016), 7**:**499. doi: 10.3389/fphar.2016.00499.
3. Casanova E, Garcia-Mina JM, Calvo MI: Antioxidant and antifungal activity of Verbena officinalis L. leaves. *Plant Foods Hum Nutr* (2008), 63**:**93-97. doi: 10.1007/s11130-008-0073-0.
4. Lopez-Jornet P, Camacho-Alonso F, Gomez-Garcia F, Molina Minano F, Canas X, Serafin A, Castillo J, Vicente-Ortega V: Effects of potassium apigenin and verbena extract on the wound healing process of SKH-1 mouse skin. *Int Wound J* (2014), 11**:**489-495. doi: 10.1111/j.1742-481X.2012.01114.x.
5. Speroni E, Cervellati R, Costa S, Guerra MC, Utan A, Govoni P, Berger A, Muller A, Stuppner H: Effects of differential extraction of Verbena officinalis on rat models of inflammation, cicatrization and gastric damage. *Planta Med* (2007), 73**:**227-235. doi: 10.1055/s-2007-967116.
6. Shu J, Chou G, Wang Z: Two new iridoids from Verbena officinalis L. *Molecules* (2014), 19**:**10473-10479. doi: 10.3390/molecules190710473.
7. Kubica P, Szopa A, Ekiert H: Production of verbascoside and phenolic acids in biomass of Verbena officinalis L. (vervain) cultured under different in vitro conditions. *Nat Prod Res*

(2017), 31:1663-1668. doi: 10.1080/14786419.2017.1286477.
8. Imran M, Salehi B, Sharifi-Rad J, Aslam Gondal T, Saeed F, Imran A, Shahbaz M, Tsouh Fokou PV, Umair Arshad M, Khan H, et al: Kaempferol: A Key Emphasis to Its Anticancer Potential. *Molecules* (2019), 24. doi: 10.3390/molecules24122277.
9. Funes L, Laporta O, Cerdan-Calero M, Micol V: Effects of verbascoside, a phenylpropanoid glycoside from lemon verbena, on phospholipid model membranes. *Chem Phys Lipids* (2010), 163:190-199. doi: 10.1016/j.chemphyslip.2009.11.004.
10. Zhao L, Liu H, Wang Y, Wang S, Xun D, Wang Y, Cheng Y, Zhang B: Multimodal Identification by Transcriptomics and Multiscale Bioassays of Active Components in Xuanfeibaidu Formula to Suppress Macrophage-Mediated Immune Response. *Engineering (Beijing)* (2021). doi: 10.1016/j.eng.2021.09.007.
11. Abel AM, Yang C, Thakar MS, Malarkannan S: Natural Killer Cells: Development, Maturation, and Clinical Utilization. *Front Immunol* (2018), 9:1869. doi: 10.3389/fimmu.2018.01869.
12. Sivori S, Vacca P, Del Zotto G, Munari E, Mingari MC, Moretta L: Human NK cells: surface receptors, inhibitory checkpoints, and translational applications. *Cell Mol Immunol* (2019), 16:430-441. doi: 10.1038/s41423-019-0206-4.
13. Schmiedel D, Mandelboim O: NKG2D Ligands-Critical Targets for Cancer Immune Escape and Therapy. *Front Immunol* (2018), 9:2040. doi: 10.3389/fimmu.2018.02040.
14. Barrow AD, Martin CJ, Colonna M: The Natural Cytotoxicity Receptors in Health and Disease. *Front Immunol* (2019), 10:909. doi: 10.3389/fimmu.2019.00909.
15. Moretta A, Bottino C, Vitale M, Pende D, Biassoni R, Mingari MC, Moretta L: Receptors for HLA class-I molecules in human natural killer cells. *Annu Rev Immunol* (1996), 14:619-648. doi: 10.1146/annurev.immunol.14.1.619.
16. Lazetic S, Chang C, Houchins JP, Lanier LL, Phillips JH: Human natural killer cell receptors involved in MHC class I recognition are disulfide-linked heterodimers of CD94 and NKG2 subunits. *J Immunol* (1996), 157:4741-4745. doi:
17. Khan M, Arooj S, Wang H: NK Cell-Based Immune Checkpoint Inhibition. *Front Immunol* (2020), 11:167. doi: 10.3389/fimmu.2020.00167.
18. Pende D, Falco M, Vitale M, Cantoni C, Vitale C, Munari E, Bertaina A, Moretta F, Del Zotto G, Pietra G, et al: Killer Ig-Like Receptors (KIRs): Their Role in NK Cell Modulation and Developments Leading to Their Clinical Exploitation. *Front Immunol* (2019), 10:1179. doi: 10.3389/fimmu.2019.01179.
19. Orange JS: Formation and function of the lytic NK-cell immunological synapse. *Nat Rev Immunol* (2008), 8:713-725. doi: 10.1038/nri2381.
20. Krzewski K, Coligan JE: Human NK cell lytic granules and regulation of their exocytosis. *Front Immunol* (2012), 3:335. doi: 10.3389/fimmu.2012.00335.
21. Osinska I, Popko K, Demkow U: Perforin: an important player in immune response. *Cent Eur J Immunol* (2014), 39:109-115. doi: 10.5114/ceji.2014.42135.
22. Chowdhury D, Lieberman J: Death by a thousand cuts: granzyme pathways of programmed cell death. *Annu Rev Immunol* (2008), 26:389-420. doi: 10.1146/annurev.immunol.26.021607.090404.
23. Kummerow C, Schwarz EC, Bufe B, Zufall F, Hoth M, Qu B: A simple, economic, time-resolved killing assay. *Eur J Immunol* (2014), 44:1870-1872. doi: 10.1002/eji.201444518.
24. Zhao R, Zhou X, Khan ES, Alansary D, Friedmann KS, Yang W, Schwarz EC, Del Campo A, Hoth M, Qu B: Targeting the Microtubule-Network Rescues CTL Killing Efficiency in Dense 3D Matrices. *Front Immunol* (2021), 12:729820. doi: 10.3389/fimmu.2021.729820.
25. Backes CS, Friedmann KS, Mang S, Knorck A, Hoth M, Kummerow C: Natural killer cells induce distinct modes of cancer cell death: Discrimination, quantification, and modulation of apoptosis, necrosis, and mixed forms. *J Biol Chem* (2018), 293:16348-16363. doi:

10.1074/jbc.RA118.004549.
26. Barrett TB, Shu G, Clark EA: CD40 signaling activates CD11a/CD18 (LFA-1)-mediated adhesion in B cells. *J Immunol* (1991), 146:1722-1729. doi:
27. Urlaub D, Hofer K, Muller ML, Watzl C: LFA-1 Activation in NK Cells and Their Subsets: Influence of Receptors, Maturation, and Cytokine Stimulation. *J Immunol* (2017), 198:1944-1951. doi: 10.4049/jimmunol.1601004.
28. Carbone E, Ruggiero G, Terrazzano G, Palomba C, Manzo C, Fontana S, Spits H, Karre K, Zappacosta S: A new mechanism of NK cell cytotoxicity activation: the CD40-CD40 ligand interaction. *J Exp Med* (1997), 185:2053-2060. doi: 10.1084/jem.185.12.2053.
29. Hill KS, Errington F, Steele LP, Merrick A, Morgan R, Selby PJ, Georgopoulos NT, O'Donnell DM, Melcher AA: OK432-activated human dendritic cells kill tumor cells via CD40/CD40 ligand interactions. *J Immunol* (2008), 181:3108-3115. doi: 10.4049/jimmunol.181.5.3108.
30. Munker R, Marini F, Jiang S, Savary C, Owen-Schaub L, Andreeff M: Expression of CD95(FAS) by gene transfer does not sensitize K562 to Fas-killing. *Hematol Cell Ther* (1997), 39:75-78. doi: 10.1007/s00282-997-0075-7.
31. Ben-Shmuel A, Sabag B, Biber G, Barda-Saad M: The Role of the Cytoskeleton in Regulating the Natural Killer Cell Immune Response in Health and Disease: From Signaling Dynamics to Function. *Front Cell Dev Biol* (2021), 9:609532. doi: 10.3389/fcell.2021.609532.
32. Qu B, Pattu V, Junker C, Schwarz EC, Bhat SS, Kummerow C, Marshall M, Matti U, Neumann F, Pfreundschuh M, et al: Docking of lytic granules at the immunological synapse in human CTL requires Vti1b-dependent pairing with CD3 endosomes. *J Immunol* (2011), 186:6894-6904. doi: 10.4049/jimmunol.1003471.
33. Zhou J, Zhang J, Lichtenheld MG, Meadows GG: A role for NF-kappa B activation in perforin expression of NK cells upon IL-2 receptor signaling. *J Immunol* (2002), 169:1319-1325. doi: 10.4049/jimmunol.169.3.1319.
34. Huang C, Bi E, Hu Y, Deng W, Tian Z, Dong C, Hu Y, Sun B: A novel NF-kappaB binding site controls human granzyme B gene transcription. *J Immunol* (2006), 176:4173-4181. doi: 10.4049/jimmunol.176.7.4173.
35. Dong W, Wu X, Ma S, Wang Y, Nalin AP, Zhu Z, Zhang J, Benson DM, He K, Caligiuri MA, Yu J: The Mechanism of Anti-PD-L1 Antibody Efficacy against PD-L1-Negative Tumors Identifies NK Cells Expressing PD-L1 as a Cytolytic Effector. *Cancer Discov* (2019), 9:1422-1437. doi: 10.1158/2159-8290.CD-18-1259.
36. Wang H, Fu C, Du J, Wang H, He R, Yin X, Li H, Li X, Wang H, Li K, et al: Enhanced histone H3 acetylation of the PD-L1 promoter via the COP1/c-Jun/HDAC3 axis is required for PD-L1 expression in drug-resistant cancer cells. *J Exp Clin Cancer Res* (2020), 39:29. doi: 10.1186/s13046-020-1536-x.
37. Vogl S, Picker P, Mihaly-Bison J, Fakhrudin N, Atanasov AG, Heiss EH, Wawrosch C, Reznicek G, Dirsch VM, Saukel J, Kopp B: Ethnopharmacological in vitro studies on Austria's folk medicine--an unexplored lore in vitro anti-inflammatory activities of 71 Austrian traditional herbal drugs. *J Ethnopharmacol* (2013), 149:750-771. doi: 10.1016/j.jep.2013.06.007.
38. Kou WZ, Yang J, Yang QH, Wang Y, Wang ZF, Xu SL, Liu J: Study on in-vivo anti-tumor activity of Verbena officinalis extract. *Afr J Tradit Complement Altern Med* (2013), 10:512-517. doi: 10.4314/ajtcam.v10i3.19.
39. Xiong WZ, Wang G, Du J, Ai W: Efficacy of herbal medicine (Xuanfei Baidu decoction) combined with conventional drug in treating COVID-19:A pilot randomized clinical trial. *Integr Med Res* (2020), 9:100489. doi: 10.1016/j.imr.2020.100489.

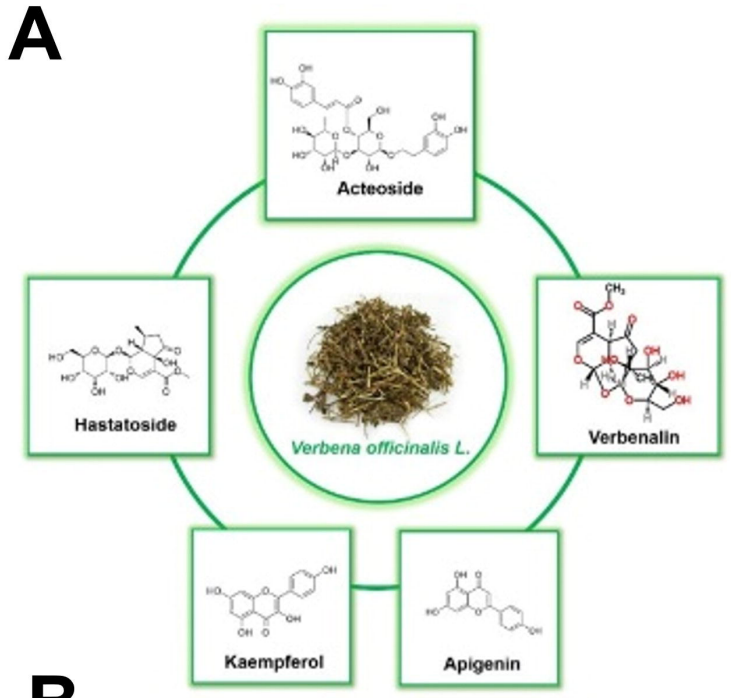
A
Acteoside
Hastatoside
Verbena officinalis L.
Verbenalin
Kaempferol
Apigenin

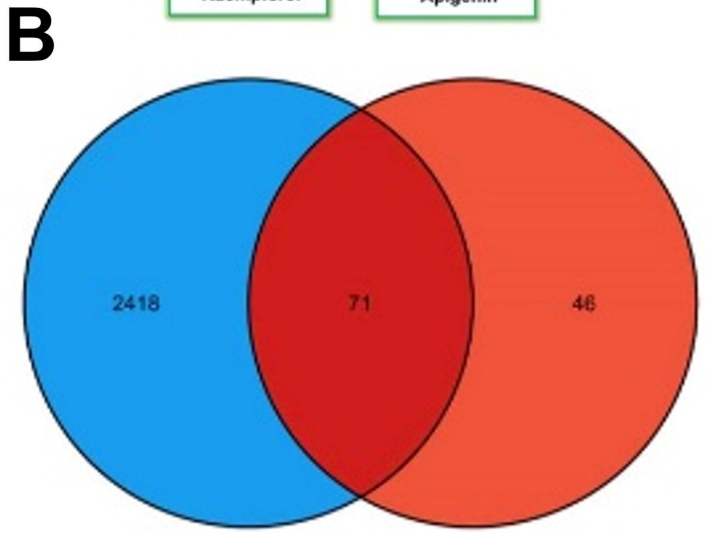
B
2418
71
46

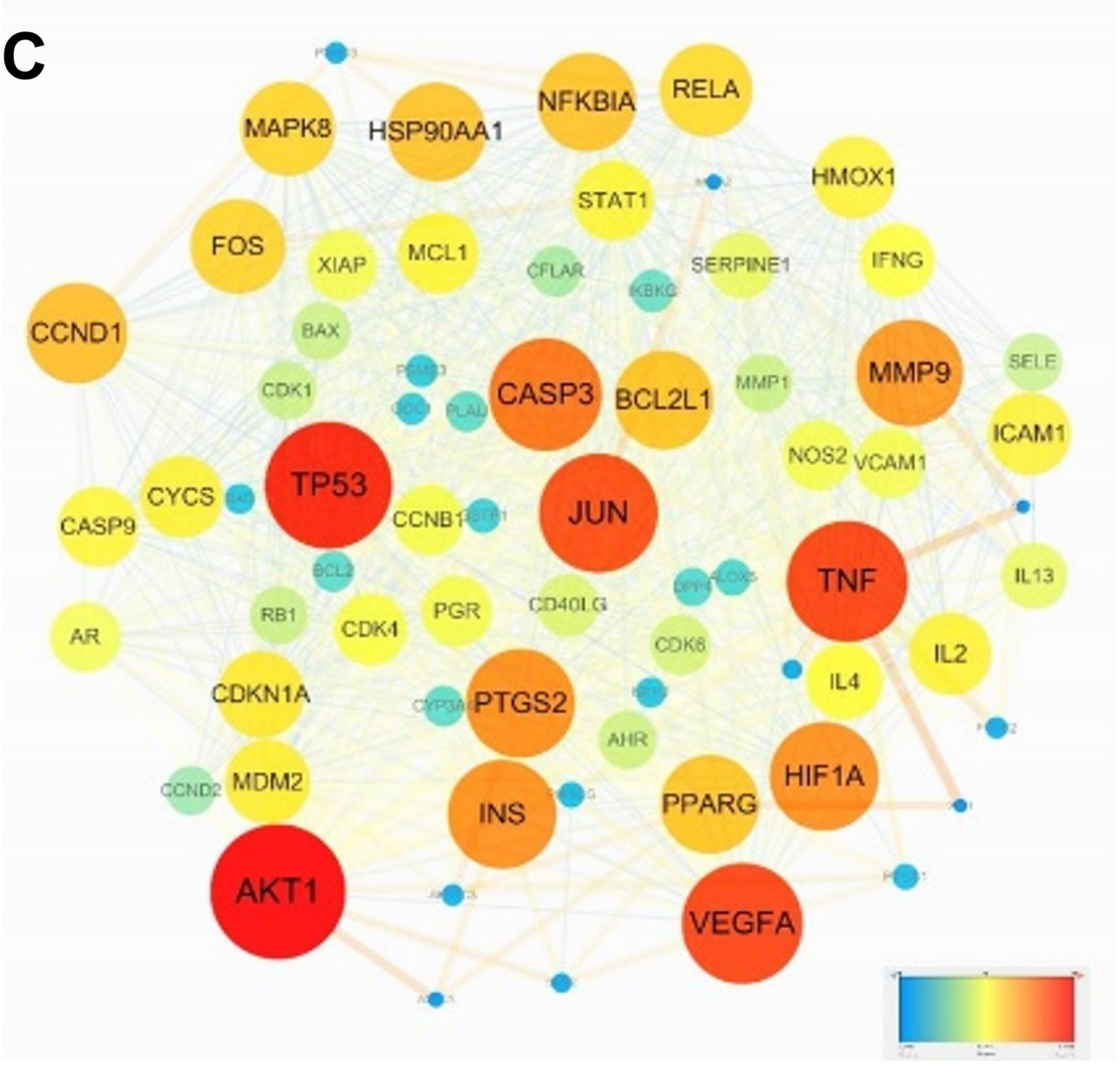
C
MAPK8
HSP90AA1
NFKBIA
RELA
HMOX1
STAT1
FOS
XIAP
MCL1
CFLAR
SERPINE1
IFNG
CCND1
BAX
CDK1
CASP3
BCL2L1
MMP1
MMP9
SELE
ICAM1
NOS2
VCAM1
TP53
CYCS
CASP9
CCNB1
JUN
TNF
IL13
AR
RB1
CDK4
PGR
CD40LG
CDK6
IL2
IL4
CDKN1A
PTGS2
AHR
HIF1A
MDM2
CCND2
INS
PPARG
AKT1
VEGFA

**A**

## NKp44

### Verbenalin

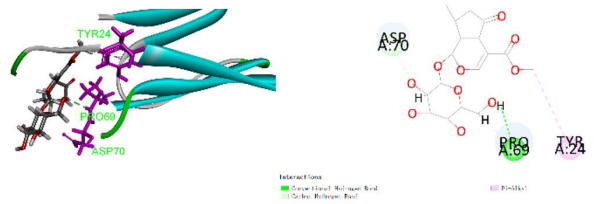

### Apigenin

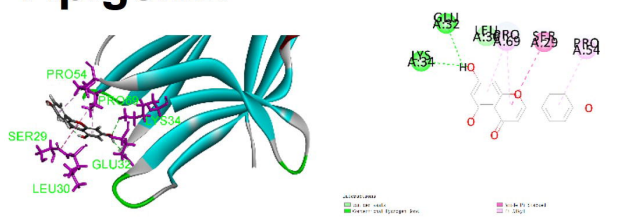

### Kaempferol

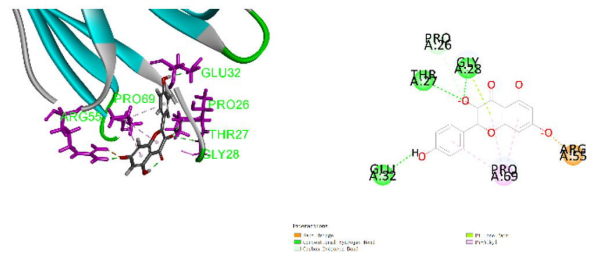

### Hastatoside

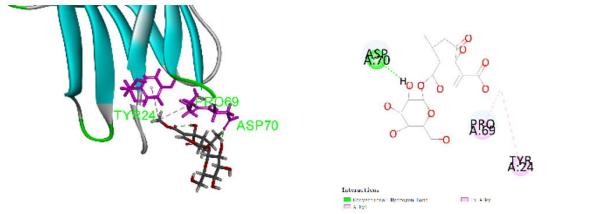

## NKp30

### Verbenalin

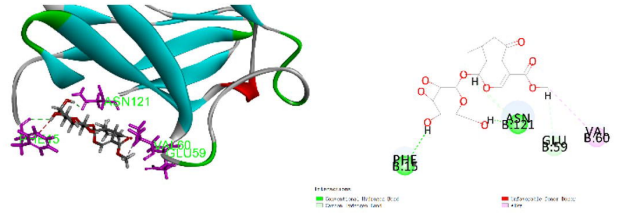

### Hastatoside

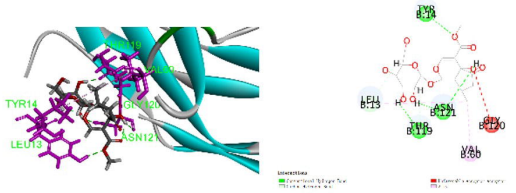

### Apigenin

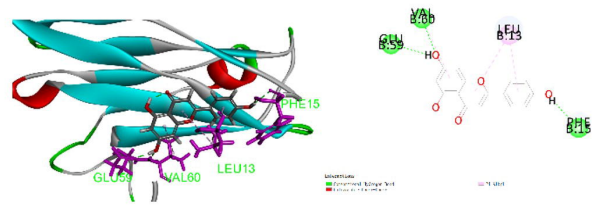

### Acteoside

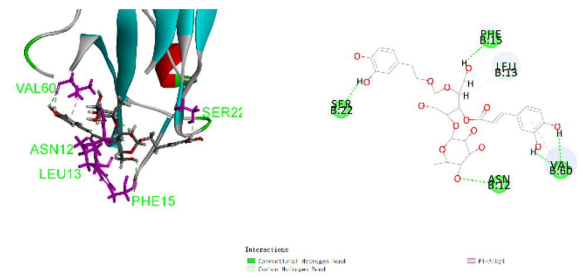

### Kaempferol

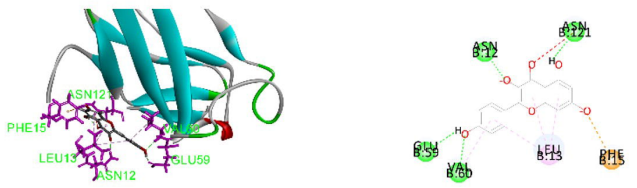

## NKG2D

### Apigenin

### Kaempferol

**B**

## NKG2A

### Verbenalin

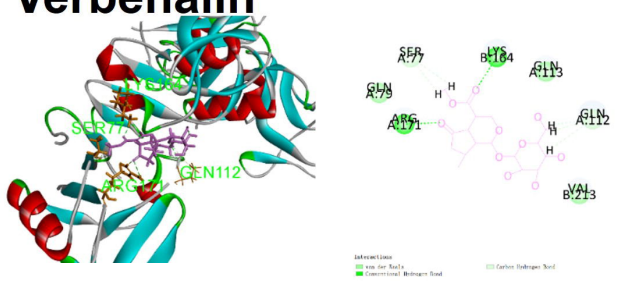

### Apigenin

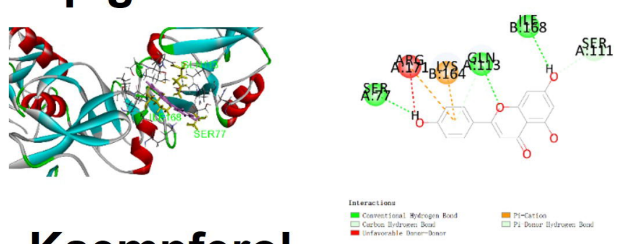

### Kaempferol

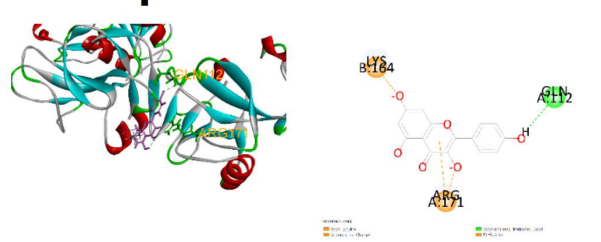

## KIR2DL1

### Verbenalin

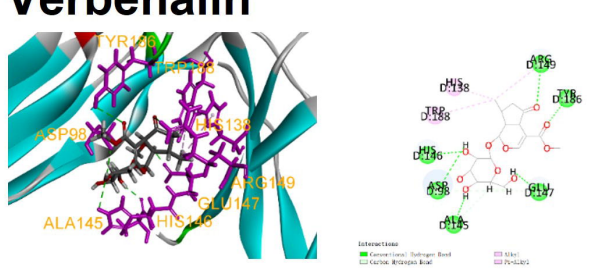

### Hastatoside

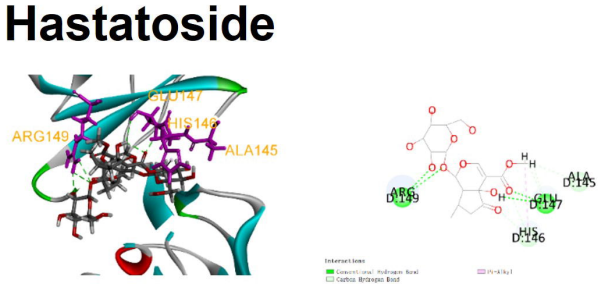

### Apigenin

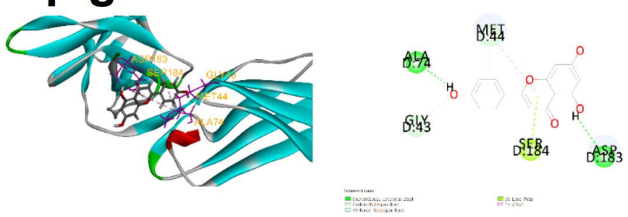

### Acteoside

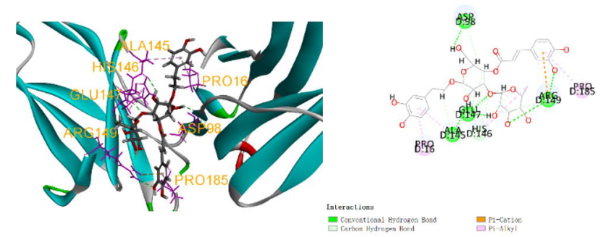

### Kaempferol

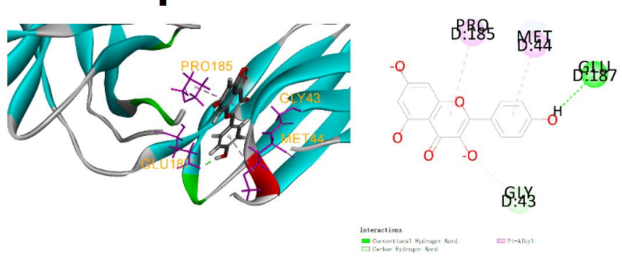

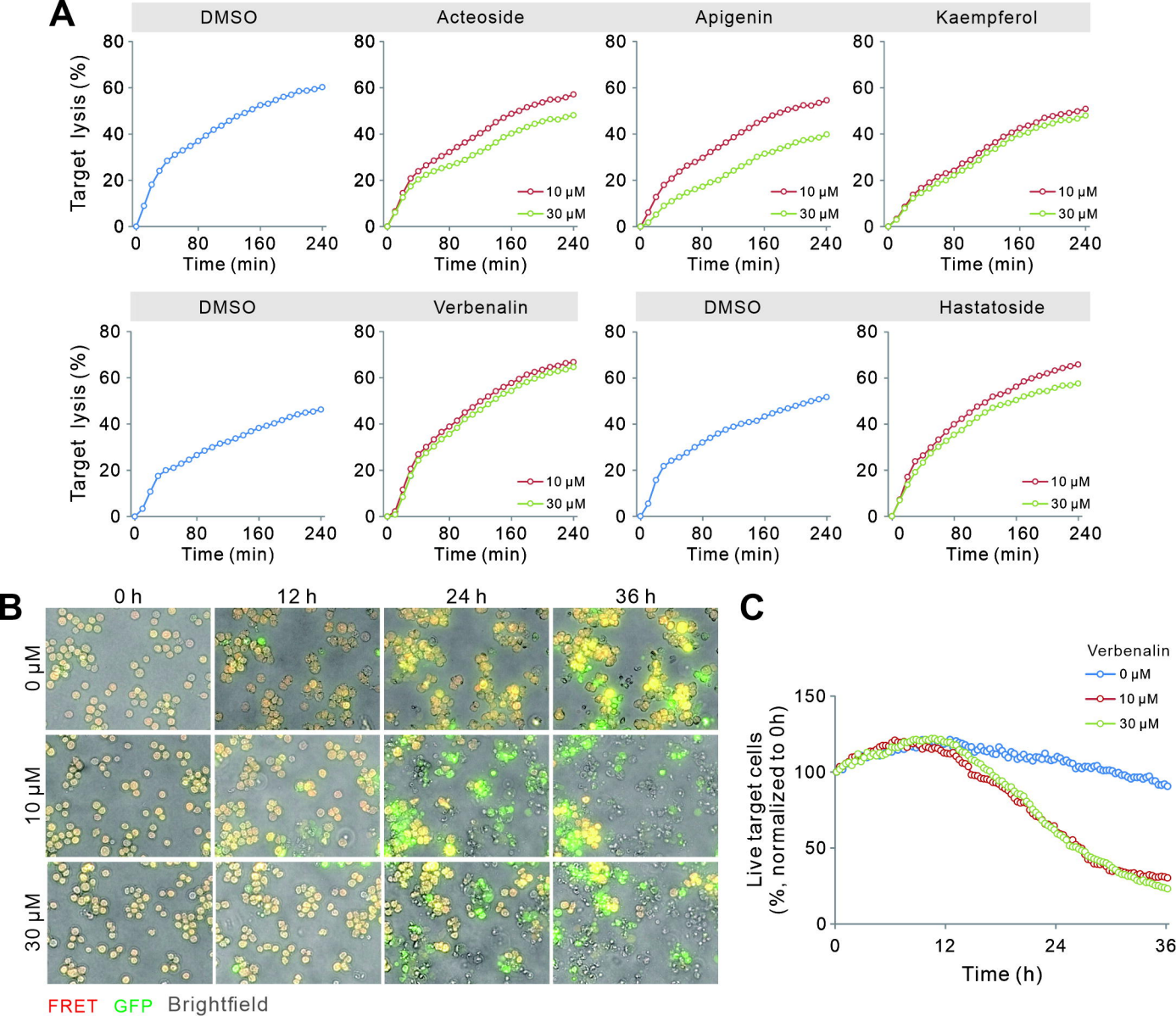
A
DMSO
Acteoside
Apigenin
Kaempferol
Verbenalin
Hastatoside
Target lysis (%)
Time (min)
10 µM
30 µM
B
0 h
12 h
24 h
36 h
0 µM
10 µM
30 µM
FRET GFP Brightfield
C
Verbenalin
0 µM
10 µM
30 µM
Live target cells
(%, normalized to 0h)
Time (h)

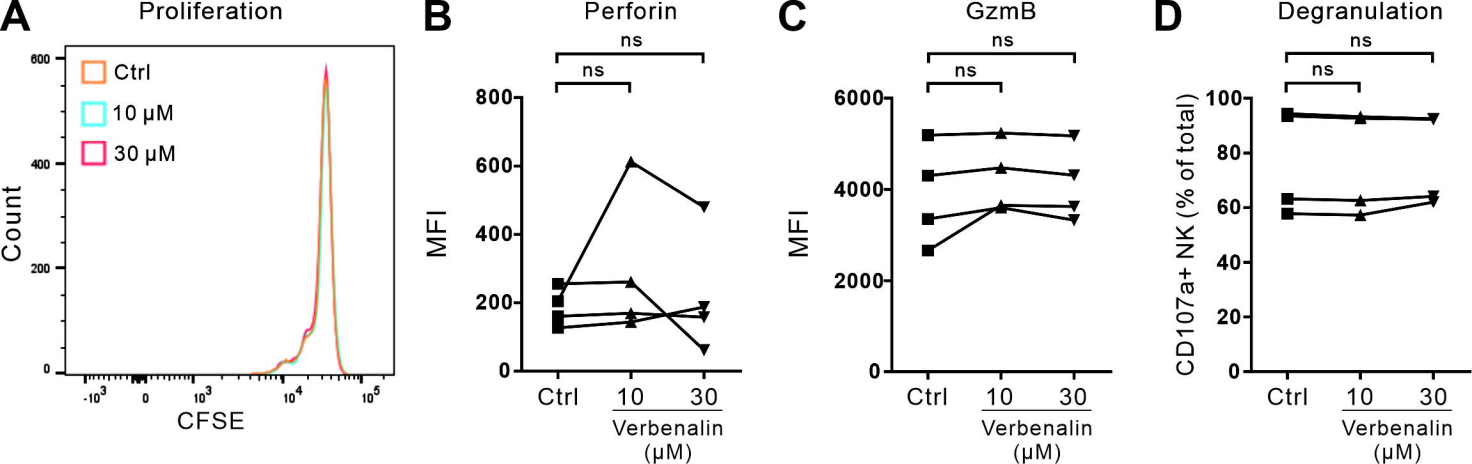
A
Proliferation
Ctrl
10 μM
30 μM
Count
CFSE
B
Perforin
ns
ns
MFI
Ctrl
10
30
Verbenalin
(μM)
C
GzmB
ns
ns
MFI
Ctrl
10
30
Verbenalin
(μM)
D
Degranulation
ns
ns
CD107a+ NK (% of total)
Ctrl
10
30
Verbenalin
(μM)

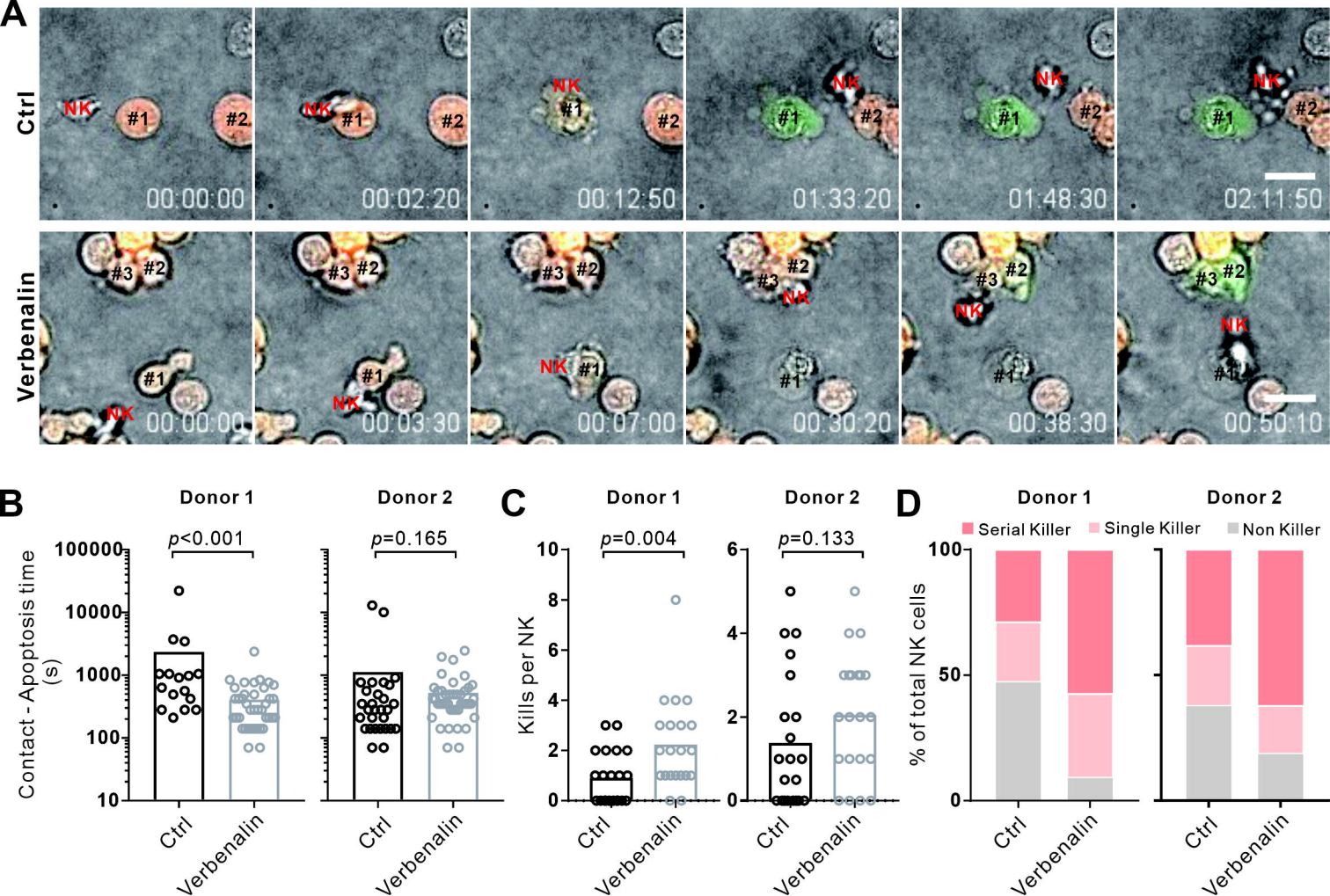
A
Ctrl
Verbenalin
NK
#1
#2
#3
00:00:00
00:02:20
00:12:50
01:33:20
01:48:30
02:11:50
00:03:30
00:07:00
00:30:20
00:38:30
00:50:10
B
Donor 1
Donor 2
p<0.001
p=0.165
Contact - Apoptosis time (s)
100000
10000
1000
100
10
Ctrl
Verbenalin
C
Donor 1
Donor 2
p=0.004
p=0.133
Kills per NK
D
Donor 1
Donor 2
Serial Killer
Single Killer
Non Killer
% of total NK cells
100
50
0